Image Cover Sheet

CLASSIFICATION	SYSTEM NUMBER
UNCLASSIFIED	149066

TITLE

INTERNAL INTERFACE CONDITIONS FOR FINITE-DIFFERENCE PE APPLICATIONS TO LAYERED ACOUSTIC MEDIA

System Number:

Patron Number:

Requester:

Notes:

DSIS Use only:

Deliver to: FF

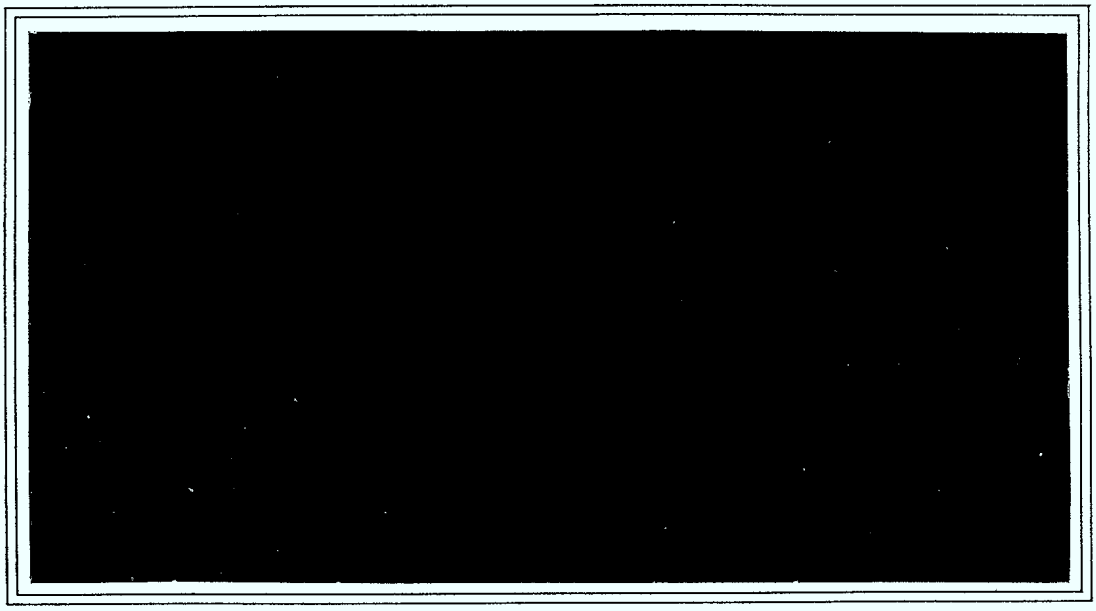

DEFENCE RESEARCH ESTABLISHMENT PACIFIC

Research and Development Branch
Department of National Defence

Canada

Defence Research Establishment Pacific

Centre de recherches pour la défense pacifique

DEFENCE RESEARCH ESTABLISHMENT PACIFIC

CFB Esquimalt, FMO Victoria, B.C. V0S 1B0

Technical Memorandum 94-145

Internal interface conditions for finite-difference PE applications to layered acoustic media

Gary H. Brooke and Philip M. Wort

December 1994

Approved By:

R P Chapman

Chief DREP

Research and Development Branch
Department of National Defence

Canada

ABSTRACT

The traditional one-way parabolic equation (PE) formulation for range-dependent layered acoustic media is modified to include effects associated with interfaces internal to the computational grid. Both first- and second-order approximations are derived which effectively translate the effects of internal boundary conditions onto nearby grid points. The approximations are based on a procedure presented by Collins [J. Acoust. Soc. Am., **86** (1989) 1459-1464] in which auxiliary field variables are defined above and below the interface. Consideration of second-order conditions also allows sloping internal interfaces to be accommodated. Numerical results obtained for standard test cases are used to demonstrate the application of the analysis. In shallow water, particularly at ranges greater than 20 km, there is an indication that precise definition of the interface depth is required in order to miminize errors that could negatively affect matched field processing applications. Alternatively, imprecision in interface location to within one computational grid width does not significantly affect the field prediction in oceans with water depths greater than 500 m or so.

1.0 Introduction

Parabolic Equation (PE) approximations to the acoustic wave equation [1] are routinely used to compute field predictions in range-dependent ocean environments. Typically, the oceanic waveguide is comprised of a finite number of horizontally-layered media separated by well defined interfaces. For example, an Arctic application might involve an ice layer floating on top of a water column which is in turn bounded below by one or more sediment layers and, finally, the basement layer. The ice/water and the water/sediment interfaces are important features and it is essential therefore that a propagation model be capable of treating these interfaces properly. Coupled-Mode [2] and Fast-Field [3] algorithms account for the exact positions of the interfaces. Finite-difference PE algorithms for layered media [4] are, in principle, also well suited to such problems. However, PE algorithms require that the field be calculated on a spatial grid of values, the simplest of which is regular in range and depth. Generally speaking, it is not possible to choose a numerically-efficient depth-grid interval which always locates a grid point exactly at the position of a physical interface.

In this paper, we describe a procedure whereby the effect of interfaces, internal to the PE computational grid, can be translated to the nearest grid points. Essentially, using a method presented by Collins [5], it is possible to derive "auxiliary" field values at grid points above and below an internal interface; proper choice of these "auxiliary" fields ensures that the boundary conditions at the internal interface are satisfied and when inserted directly into the PE algorithm serve effectively to distribute the effect of the internal interface onto the computational grid. Moreover, it is possible to extend the analysis to include higher-order terms to accommodate sloping interfaces which are internal to the computational grid. Inclusion of higher-order terms causes the tridiagonal form of the matrices, associated with the PE solution, to be altered locally in the two rows that correspond to the position of the interface. Fortunately, it is a simple matter to transform these matrices back to the preferred tridiagonal form. Consequently, range-dependence can be handled using standard range-updating procedures. As such, the efficiency of the PE calculations is not significantly affected. Computations using an Implicit Finite Difference PE algorithm, **GHBPE** [6], modified to account for the exact position of internal

interfaces indicate, not surprisingly, that in deep water the propagation is not very sensitive to the position of the interface. In shallow water, the effects can be more significant.

The manuscript is organized in the following manner. Initially, a brief description of the **GHBPE** algorithm used for range-independent acoustic media is presented. Then, both first- and second-order internal interface conditions are derived and an anlaysis is presented which indicates how the conditions translate onto the PE grid. Second-order conditions allow sloping interfaces to be accommodated, thus a brief description is given of the associated mathematical development. Finally, the resultant algorithms are applied to some simple test cases in order to illustrate the effects.

2.0 GHBPE: Range-Independent Layered Media

Consider the two-dimensional layered acoustic structure bounded above and below by perfect reflecting surfaces illustrated in Figure 1. We define the three major components of the waveguide to be (i) a water column, (ii) an ocean bottom and (iii) a bottom absorbing region. Initially, for analysis purposes, we do not allow range-dependence within the waveguide; subsequently, we allow the medium to change at each range step. Generally speaking, PE algorithms are derived by discretizing the governing equations in terms of field quantities defined on a grid of points overlaying the waveguide (here we

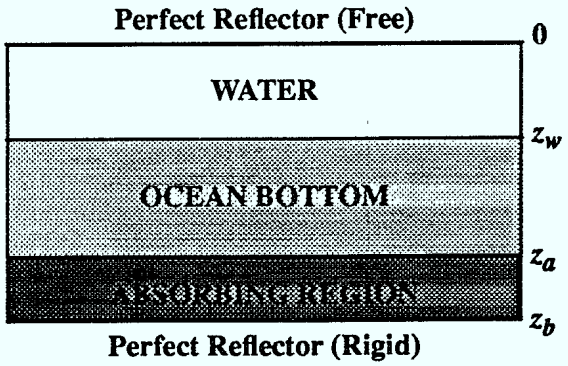

FIGURE 1. Layered acoustic structure.

consider a two-dimensional grid in range and depth). **GHBPE** accomplishes this using a Crank-Nicolson [7] discretization scheme for the range-coordinate and a layered waveguide approach [4] to the depth discretization in which the water column, the ocean bottom and the bottom absorbing region are each subdivided into many homogeneous layers. As is common to most acoustic PE algorithms, the field quantities on the grid can be marched in range by solving a tridiagonal matrix at each range step.

2.1 Basic Equations

Within each homogeneous layer comprising the discretized waveguide, we require that the acoustic pressure, $p(x,z)$, satisfy the Helmholtz equation

$$\left\{\frac{\partial^2}{\partial x^2} + \frac{\partial^2}{\partial z^2} + k_o^2 n^2(z)\right\} p(x,z) = 0 \ . \tag{1}$$

In the following analysis, we restrict our attention to a two-dimensional (2-D) waveguide in a Cartesian coordinate system. In equation (1), k_o is a reference wavenumber and $n^2(z)$, the refractive index profile for the medium, is constant within each of the PE grid layers. For range-independent media, equation (1) can be factored into two first-order parabolic equations in the range coordinate representing forward and backward propagation. Here we restrict the discussion to the forward propagating field component, $\vec{p}(x,z)$, which satisfies

$$\frac{\partial}{\partial x}\vec{p}(x,z) = ik_o Q^{1/2}(z)\vec{p}(x,z) \tag{2}$$

where

$$Q^{1/2}(z) = \left\{\frac{1}{k_o^2}\frac{\partial^2}{\partial z^2} + n^2(z)\right\}^{1/2} \tag{3}$$

is a pseudo-differential square-root operator. For numerical purposes we define a PE computational field, $\psi(x,z)$, which is proportional to the forward-going pressure (for

convenience we drop the arrow notation with the understanding that ψ and p represent forward propagating fields) but with rapidly oscillating phase component removed (i.e., $p(x, z) = e^{ik_o x} \psi(x, z)$). Then

$$\frac{\partial}{\partial x}\psi(x, z) = ik_o\{Q^{1/2}(z) - 1\}\psi(x, z) \quad . \tag{4}$$

The **GHBPE** algorithm is concerned with the numerical solution of equation (4). One problem encountered is the representation of the square-root operator. Here, in this analysis, we use a rational-linear approximation given by

$$Q^{1/2}(z) \approx 1 + \frac{a_1\{1 - Q(z)\}}{1 + b_1 Q(z)} = 1 + F_1(Q(z)) \quad . \tag{5}$$

In practise, an n^{th}-order Padé expansion (a sum of "n" rational linear terms) with complex coefficients is used in the numerical implementation of **GHBPE**.

2.2 Range Discretization

Consider the Taylor approximation for the forward propagating field given by

$$\psi(x + \Delta x, z) = e^{\Delta x \partial x}\psi(x, z) \quad . \tag{6}$$

Let us substitute from equation (4) and (5) to obtain

$$\psi(x + \Delta x, z) = e^{ik_o \Delta x F_1(Q(z))}\psi(x, z) \quad . \tag{7}$$

Following the usual Crank-Nicolson procedure, equation (7) can be cast in the following implicit form

$$\left\{A_2\frac{\partial^2}{\partial z^2} + B_2\right\}\psi(x + \Delta x, z) = \left\{A_1\frac{\partial^2}{\partial z^2} + B_1\right\}\psi(x, z) \tag{8}$$

where

$$A_2 = b_1 + \frac{ik_o\Delta x}{2}a_1$$

$$A_1 = b_1 - \frac{ik_o\Delta x}{2}a_1$$

$$B_2 = k_o^2\left\{ 1 - \frac{ik_o\Delta x}{2}a_1 + A_2 n^2(z) \right\}$$

$$B_1 = k_o^2\left\{ 1 + \frac{ik_o\Delta x}{2}a_1 + A_1 n^2(z) \right\} \quad . \tag{9}$$

Equation (8) represents the basic propagation equation for the PE fields.

2.3 Depth Discretization

As mentioned previously, discretization in depth is realized by dividing the waveguide into many horizontally stratified homogeneous layers. Having defined the layers, the boundary conditions at the interfaces between those layers must be satisfied. Consider the layered medium shown in Figure 2. The boundary conditions at the j^{th} interface are (superscripts "$\mp$" refer to "above/below" the interface respectively)

$$\psi_{1,j}^{-} = \psi_{1,j}^{+} \tag{10}$$

and

$$\frac{1}{\rho_j}\frac{\partial}{\partial z}\left(\psi_{1,j}^{-}\right) = \frac{1}{\rho_{j+1}}\frac{\partial}{\partial z}\left(\psi_{1,j}^{+}\right) \tag{11}$$

at the advanced range step, $x=x_2=x_1+\Delta x$. The PE fields may be expanded using the second-order accurate, first-order difference formulas [4] as

$$\frac{\partial}{\partial z}\left(\psi_{1,j}^{-}\right) = \frac{\psi_{1,j}^{-} - \psi_{1,j-1}^{+}}{\Delta z} + \frac{\Delta z}{6}\left\{\frac{\partial^2}{\partial z^2}\left(\psi_{1,j-1}^{+}\right) + 2\frac{\partial^2}{\partial z^2}\left(\psi_{1,j}^{-}\right)\right\} \tag{12}$$

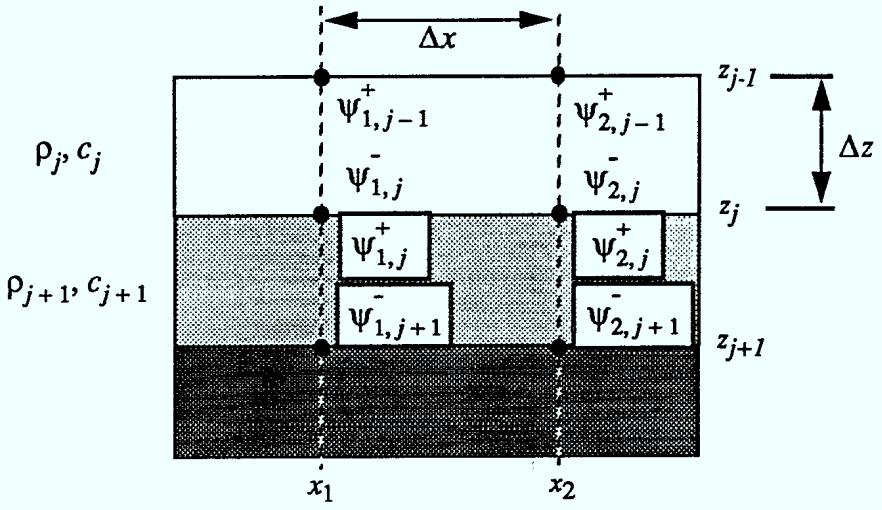

FIGURE 2. Layered waveguide system.

and

$$\frac{\partial}{\partial z}\left(\Psi^{+}_{1,j}\right) = \frac{\Psi^{-}_{1,j+1} - \Psi^{+}_{1,j}}{\Delta z} - \frac{\Delta z}{6}\left\{\frac{\partial^2}{\partial z^2}\left(\Psi^{-}_{1,j+1}\right) + 2\frac{\partial^2}{\partial z^2}\left(\Psi^{+}_{1,j}\right)\right\} \tag{13}$$

at $x=x_1$ and, similarly at $x=x_2$. Now substituting these expansions into the boundary conditions and making use of equation (8) to eliminate the second-derivative terms yields the following relationship for the j^{th} interface (i.e., the j^{th} grid point)

$$m^{l}_{1j}\Psi_{2,j-1} + m^{l}_{2j}\Psi_{2,j} + m^{l}_{3j}\Psi_{2,j+1} = m^{r}_{1j}\Psi_{1,j-1} + m^{r}_{2j}\Psi_{1,j} + m^{r}_{3j}\Psi_{1,j+1} \tag{14}$$

where (for $j=2,..,N-1$)

$$\begin{aligned} m^{l}_{1j} &= -\rho_{j+1}\left\{\frac{A_2}{\Delta z} + \frac{\Delta z B^{j}_{2}}{6}\right\} \\ m^{l}_{2j} &= \{\rho_{j+1} + \rho_j\}\frac{A_2}{\Delta z} - \rho_{j+1}\frac{\Delta z B^{j}_{2}}{3} - \rho_j\frac{\Delta z B^{j+1}_{2}}{3} \\ m^{l}_{3j} &= -\rho_j\left\{\frac{A_2}{\Delta z} + \frac{\Delta z B^{j+1}_{2}}{6}\right\} \end{aligned} \tag{15}$$

and

$$
\begin{aligned}
m_{1j}^{r} &= -\rho_{j+1}\left\{\frac{A_1}{\Delta z}+\frac{\Delta z B_1^{j}}{6}\right\} \\
m_{2j}^{r} &= \{\rho_{j+1}+\rho_j\}\frac{A_1}{\Delta z}-\rho_{j+1}\frac{\Delta z B_1^{j}}{3}-\rho_j\frac{\Delta z B_1^{j+1}}{3} \\
m_{3j}^{r} &= -\rho_j\left\{\frac{A_1}{\Delta z}+\frac{\Delta z B_1^{j+1}}{6}\right\} \quad .
\end{aligned}
\tag{16}
$$

Note that in equation (14), we have dropped the superscripts on the PE fields due to their continuity across layer interfaces.

Equation (14) can be written for every grid point in depth (i.e., at every interface) in the waveguide. An implicit assumption here is that all interfaces lie on grid points - as such, equation (14) applies equally well to the water/bottom interface. Of course, some slight modifications take effect at the grid points on or near a waveguide boundary. Specifically, at the free surface, $z=0$, we do not specify a grid point at this depth but rather use a zero-value of the field. Therefore, the equation for the uppermost grid point (i.e., $j=1$) is

$$
m_{21}^{l}\Psi_{2,1}+m_{31}^{l}\Psi_{2,2} = m_{21}^{r}\Psi_{1,1}+m_{31}^{r}\Psi_{1,2} \quad . \tag{17}
$$

Conversely, at the lower rigid boundary, $z=z_B$, we do locate a grid point. Moreover, we enforce the boundary condition that the normal derivative must vanish by making the field and the medium even about the rigid surface. Thus, the equation for the lowermost grid point (i.e., j=N) is given by

$$
m_{1N}^{l}\Psi_{2,N-1}+m_{2N}^{l}\Psi_{2,N} = m_{1N}^{r}\Psi_{1,N-1}+m_{2N}^{r}\Psi_{1,N} \tag{18}
$$

where

$$
\begin{aligned}
m_{1N}^{l} &= -\rho_N\left\{\frac{A_2}{\Delta z}+\frac{\Delta z B_2^{N}}{6}\right\} \\
m_{2N}^{l} &= \rho_N\left\{\frac{A_2}{\Delta z}-\frac{\Delta z B_2^{N}}{3}\right\}
\end{aligned}
\tag{19}
$$

and

$$m^r_{1N} = -\rho_N \left\{ \frac{A_1}{\Delta z} + \frac{\Delta z B_1^N}{6} \right\}$$
$$m^r_{2N} = \rho_N \left\{ \frac{A_1}{\Delta z} - \frac{\Delta z B_1^N}{3} \right\} \quad . \tag{20}$$

The result of combining equation (14) at all of the layer interfaces (including equations (17) and (18) at the top and bottom grid points) is a tridiagonal matrix system of equations for the fields at the advanced range step in terms of the fields at the current range step. In matrix form, the forward propagating fields satisfy

$$M_L \underline{\Psi}^+_2 (x + \Delta x) = M_R \underline{\Psi}^+_1 (x) \tag{21}$$

where M_L and M_R are tridiagonal ***marching matrices*** with elements defined by

$$M_L = \begin{bmatrix} m^l_{21} & m^l_{31} & 0 & 0 & 0 & 0 & 0 & 0 & 0 \\ m^l_{12} & m^l_{22} & m^l_{32} & 0 & 0 & 0 & 0 & 0 & 0 \\ 0 & \cdot & \cdot & \cdot & 0 & 0 & 0 & 0 & 0 \\ 0 & 0 & \cdot & \cdot & \cdot & 0 & 0 & 0 & 0 \\ 0 & 0 & 0 & m^l_{1j} & m^l_{2j} & m^l_{3j} & 0 & 0 & 0 \\ 0 & 0 & 0 & 0 & m^l_{1j+1} & m^l_{2j+1} & m^l_{3j+1} & 0 & 0 \\ 0 & 0 & 0 & 0 & 0 & \cdot & \cdot & \cdot & 0 \\ 0 & 0 & 0 & 0 & 0 & 0 & \cdot & \cdot & \cdot \\ 0 & 0 & 0 & 0 & 0 & 0 & 0 & m^l_{1N-1} & m^l_{2N} \end{bmatrix} \tag{22}$$

and

$$M_R = \begin{bmatrix} m_{21}^r & m_{31}^r & 0 & 0 & 0 & 0 & 0 & 0 & 0 \\ m_{12}^r & m_{22}^r & m_{32}^r & 0 & 0 & 0 & 0 & 0 & 0 \\ 0 & \cdot & \cdot & \cdot & 0 & 0 & 0 & 0 & 0 \\ 0 & 0 & \cdot & \cdot & \cdot & 0 & 0 & 0 & 0 \\ 0 & 0 & 0 & m_{1j}^r & m_{2j}^r & m_{3j}^r & 0 & 0 & 0 \\ 0 & 0 & 0 & 0 & m_{1j+1}^r & m_{2j+1}^r & m_{3j+1}^r & 0 & 0 \\ 0 & 0 & 0 & 0 & 0 & \cdot & \cdot & \cdot & 0 \\ 0 & 0 & 0 & 0 & 0 & 0 & \cdot & \cdot & \cdot \\ 0 & 0 & 0 & 0 & 0 & 0 & 0 & m_{1N-1}^r & m_{2N}^r \end{bmatrix} . \quad (23)$$

In equation (21), $\underline{\Psi}_2^+(x+\Delta x)$ and $\underline{\Psi}_1^+(x)$ are vectors whose elements are the PE field values on the grid points in depth at the advanced range step and at the current range step respectively.

In this section we have outlined the basic analysis associated with the marching scheme used in **GHBPE** for range-independent acoustic waveguides. That is, the PE field is marched by successively solving the tridiagonal matrix system in equation (21) at each range step. The starting field (i.e., at $x=0$) may be any one of a number of straightforward choices ranging from a simple Gaussian function of depth [8] to a state-of-the-art Collins starter [9].

2.4 Interface between grid points (first-order approximation)

The finite-difference analysis presented thus far assumes that all horizontal interfaces lie directly on the discretization grid. This may be adequate for those layers within the water column or within the bottom because we are able to choose the depth grid to be a specific value independent of water depth or bottom thickness. A problem occurs when the water-bottom interface lies between grid points. The current version of

GHBPE adjusts the interface depth such that it lies on the closest grid point - a simple but restrictive solution. Recently, Collins [5] showed that it was possible to mimic the effect of an internal interface by defining auxiliary field values above and below the interface. These values reflect approximately the boundary conditions found at the internal interface and allow the usual matrix equations to be applied at each grid point. Here we show that the same analysis can be extended to layered problems where forward/backward differences are used in the discretization procedure. Consider the internal interface at $z=z_b$ ($z_j<z_b<z_{j+1}$) illustrated in the central portion of Figure 3. Note that we have continued medium "j" down to the internal interface from above and continued medium "j+1" up to the internal interface from below. In the left hand configuration, we define an auxiliary field value ψ^a_{j+1} at the grid point below the interface. This auxiliary field value is treated as is if it were contained wholly within medium "*j*" (i.e., effectively we have continued medium "*j*" down to the $j+1^{\text{th}}$ grid level as if the internal interface did not exist). Then, in terms of the value of the field just above the interface, ψ_b^-, we can write Taylor expansions to first order as

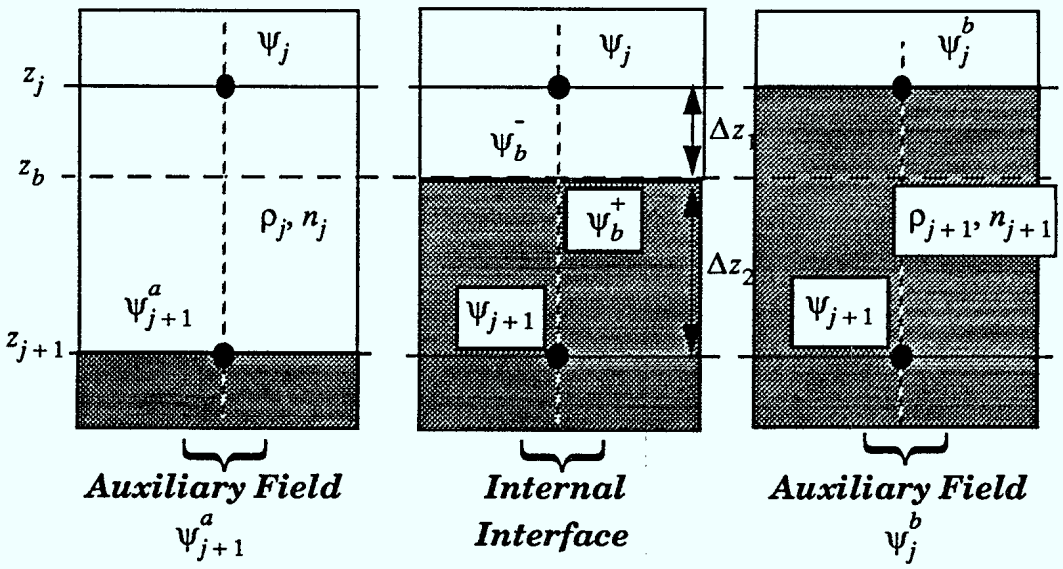

FIGURE 3. Auxiliary field definition for an internal interface (first-order). The range subscript has been suppressed.

$$\psi_{1,j} = \bar{\psi}_{1,b} - \Delta z_1 \frac{\partial \bar{\psi}_{1,b}}{\partial z} \tag{24}$$

and

$$\psi^a_{1,j+1} = \bar{\psi}_{1,b} + \Delta z_2 \frac{\partial \bar{\psi}_{1,b}}{\partial z} \tag{25}$$

in which case,

$$\bar{\psi}_{1,b} = \frac{\Delta z_2}{\Delta z}\psi_{1,j} + \frac{\Delta z_1}{\Delta z}\psi^a_{1,j+1} \tag{26}$$

and

$$\frac{\partial \bar{\psi}_{1,b}}{\partial z} = \frac{\psi^a_{1,j+1} - \psi_{1,j}}{\Delta z} \ . \tag{27}$$

where $\Delta z = \Delta z_1 + \Delta z_2$ (note that subscript "1" on the PE field quantities refers to the range x_1). Similarly, we define (see the configuration on the right hand side of Figure 3) an auxiliary field value $\psi^b_{1,j}$ at the grid point above the interface. We treat this auxiliary value as if the interface did not exist and as if the medium were wholly comprised of medium "*j+1*". Then

$$\psi^b_{1,j} = \psi^+_{1,b} - \Delta z_1 \frac{\partial \psi^+_{1,b}}{\partial z} \tag{28}$$

and

$$\psi_{1,j+1} = \psi^+_{1,b} + \Delta z_2 \frac{\partial \psi^+_{1,b}}{\partial z} \tag{29}$$

in which case,

$$\psi^+_{1,b} = \frac{\Delta z_2}{\Delta z}\psi^b_{1,j} + \frac{\Delta z_1}{\Delta z}\psi_{1,j+1} \tag{30}$$

and

$$\frac{\partial \psi^{+}_{1,b}}{\partial z} = \frac{\psi_{1,j+1} - \psi^{b}_{1,j}}{\Delta z} \quad . \tag{31}$$

The boundary conditions at the internal interface require continuity of pressure and normal displacement. Thus,

$$\bar{\psi}_{1,b} = \psi^{+}_{1,b} \tag{32}$$

and

$$\frac{1}{\rho_j}\left\{\frac{\partial \bar{\psi}_{1,b}}{\partial z}\right\} = \frac{1}{\rho_{j+1}}\left\{\frac{\partial \psi^{+}_{1,b}}{\partial z}\right\} \quad . \tag{33}$$

Using equations (26), (27), (30) and (31) we can write the following system for the auxilary fields, namely

$$\begin{aligned} \Delta z_2 \psi^{b}_{1,j} - \Delta z_1 \psi^{a}_{1,j+1} &= \Delta z_2 \psi_{1,j} - \Delta z_1 \psi_{1,j+1} \\ \rho_j \psi^{b}_{1,j} + \rho_{j+1} \psi^{a}_{1,j+1} &= \rho_{j+1} \psi_{1,j} + \rho_j \psi_{1,j+1} \end{aligned} \tag{34}$$

in which case

$$\psi^{a}_{1,j+1} = \alpha_j \psi_{1,j} + \alpha_{j+1} \psi_{1,j+1} \tag{35}$$

and

$$\psi^{b}_{1,j} = \beta_j \psi_{1,j} + \beta_{j+1} \psi_{1,j+1} \tag{36}$$

where

$$\begin{aligned} \alpha_j &= \frac{1}{\Omega}\{\rho_{j+1} - \rho_j\}\Delta z_2 \\ \alpha_{j+1} &= \frac{1}{\Omega}\rho_j \Delta z \\ \beta_j &= \frac{1}{\Omega}\rho_{j+1}\Delta z \\ \beta_{j+1} &= -\frac{1}{\Omega}\{\rho_{j+1} - \rho_j\}\Delta z_1 \end{aligned} \tag{37}$$

and $\Omega = \rho_{j+1}\Delta z_2 + \rho_j \Delta z_1$.

Similarly, at the advanced range step (i.e., $x = x_2$) we have

$$\psi^a_{2,j+1} = \alpha_j \psi_{2,j} + \alpha_{j+1}\psi_{2,j+1} \tag{38}$$

and

$$\psi^b_{2,j} = \beta_j \psi_{2,j} + \beta_{j+1}\psi_{2,j+1} \ . \tag{39}$$

These expressions for the auxiliary fields can be substituted directly into equation (14) to yield "auxiliary" equations for the grid points just above and just below the interface. That is, just above the internal interface (i.e., at the j^{th} grid point) we have

$$m^l_{1j}\psi_{2,j-1} + m^l_{2j}\psi_{2,j} + m^l_{3j}\psi^a_{2,j+1} = m^r_{1j}\psi_{1,j-1} + m^r_{2j}\psi_{1,j} + m^r_{3j}\psi^a_{1,j+1} \tag{40}$$

or using equations (35) and (38)

$$\begin{aligned} m^l_{1j}\psi_{2,j-1} + \{m^l_{2j} + m^l_{3j}\alpha_j\}\psi_{2,j} + m^l_{3j}\alpha_{j+1}\psi_{2,j+1} = \\ m^r_{1j}\psi_{1,j-1} + \{m^r_{2j} + m^r_{3j}\alpha_j\}\psi_{1,j} + m^r_{3j}\alpha_{j+1}\psi_{1,j+1} \ . \end{aligned} \tag{41}$$

Similarly, just below the internal interface (i.e. at the $j+1^{\text{th}}$ grid point) we use equations (36) and (39) to obtain

$$\begin{aligned} m^l_{1j+1}\psi^b_{2,j} + m^l_{2j+1}\psi_{2,j+1} + m^l_{3j+1}\psi_{2,j+2} = \\ m^r_{1j+1}\psi^b_{1,j} + m^r_{2j+1}\psi_{1,j+1} + m^r_{3j+1}\psi_{1,j+2} \end{aligned} \tag{42}$$

and hence

$$\begin{aligned} m^l_{1j+1}\beta_j\psi_{2,j} + \{m^l_{2j+1} + m^l_{1j+1}\beta_{j+1}\}\psi_{2,j+1} + m^l_{3j+1}\psi_{2,j+2} = \\ m^r_{1j+1}\beta_j\psi_{1,j} + \{m^r_{2j+1} + m^r_{1j+1}\beta_{j+1}\}\psi_{1,j+1} + m^r_{3j+1}\psi_{1,j+2} \ . \end{aligned} \tag{43}$$

Equations (41) and (43) can be used directly to modify the j^{th} and $j+1^{th}$ rows of the marching matrices in equations (22) and (23). Thus, with only a few slight modifications to the marching matrix elements (corresponding to the grid points nearest the internal interface) the effect of an internal interface can be incorporated straightforwardly into the basic **GHBPE** algorithm.

2.5 Interface between grid points (second-order approximation)

The analysis of the previous section provides a means of incorporating the boundary conditions at an interface which lies between grid points while maintaining the traditional tridiagonal form of the matrices used in the PE marching algorithm. It is important to note that the tridiagonal form is assured only if first-order approximations are used in defining the field and its depth derivative on the interface. If we are prepared to relax the constraint that the matrices be tridiagonal, we can achieve a formulation which is second-order accurate (as will be apparent, however, it will be extremely easy to retridiagonalize the matrices). Second-order accuracy for the internal interface is considered here for two reasons, namely (i) it seems reasonable to make the internal interface computations more consistent with the second-order accurate forward/backward differences associated with all other layer interfaces, and (ii) it leads naturally to a formulation which allows sloping interface conditions to be accommodated (discussed in the next section). Consider the section of waveguide illustrated in Figure 4 with an interface which lies between the PE grid. We again define auxiliary fields, $\psi^{a}_{1,j+1}$ and $\psi^{b}_{1,j}$, but we are going to demand that second-order accuracy be maintained. Proceeding as before, we define the following relationships (at $x = x_1$):

$$\psi_{1,j} = \bar{\psi}_{1,b} - \Delta z_1 \frac{\partial \bar{\psi}_{1,b}}{\partial z} + \frac{\{\Delta z_1\}^2}{2} \frac{\partial^2 \bar{\psi}_{1,b}}{\partial z^2}, \tag{44}$$

$$\psi_{1,j-1} = \bar{\psi}_{1,b} - \{\Delta z + \Delta z_1\} \frac{\partial \bar{\psi}_{1,b}}{\partial z} + \frac{\{\Delta z + \Delta z_1\}^2}{2} \frac{\partial^2 \bar{\psi}_{1,b}}{\partial z^2} \tag{45}$$

and

$$\psi^{a}_{1,j+1} = \bar{\psi}_{1,b} + \Delta z_2 \frac{\partial \bar{\psi}_{1,b}}{\partial z} + \frac{\{\Delta z_2\}^2}{2} \frac{\partial^2 \bar{\psi}_{1,b}}{\partial z^2}. \tag{46}$$

Equations (44-46) represent three equations in three unknown field quantities at the interface, namely $\bar{\psi}_{1,b}$, $\partial\bar{\psi}_{1,b}/\partial z$ and $\partial^2\bar{\psi}_{1,b}/\partial z^2$. Note that the second-order accuracy implicit in the expansions (44-46) is slightly different than that found in equations (12-13) because third-order adjustments (contained in equations (12-13)) have been excluded.

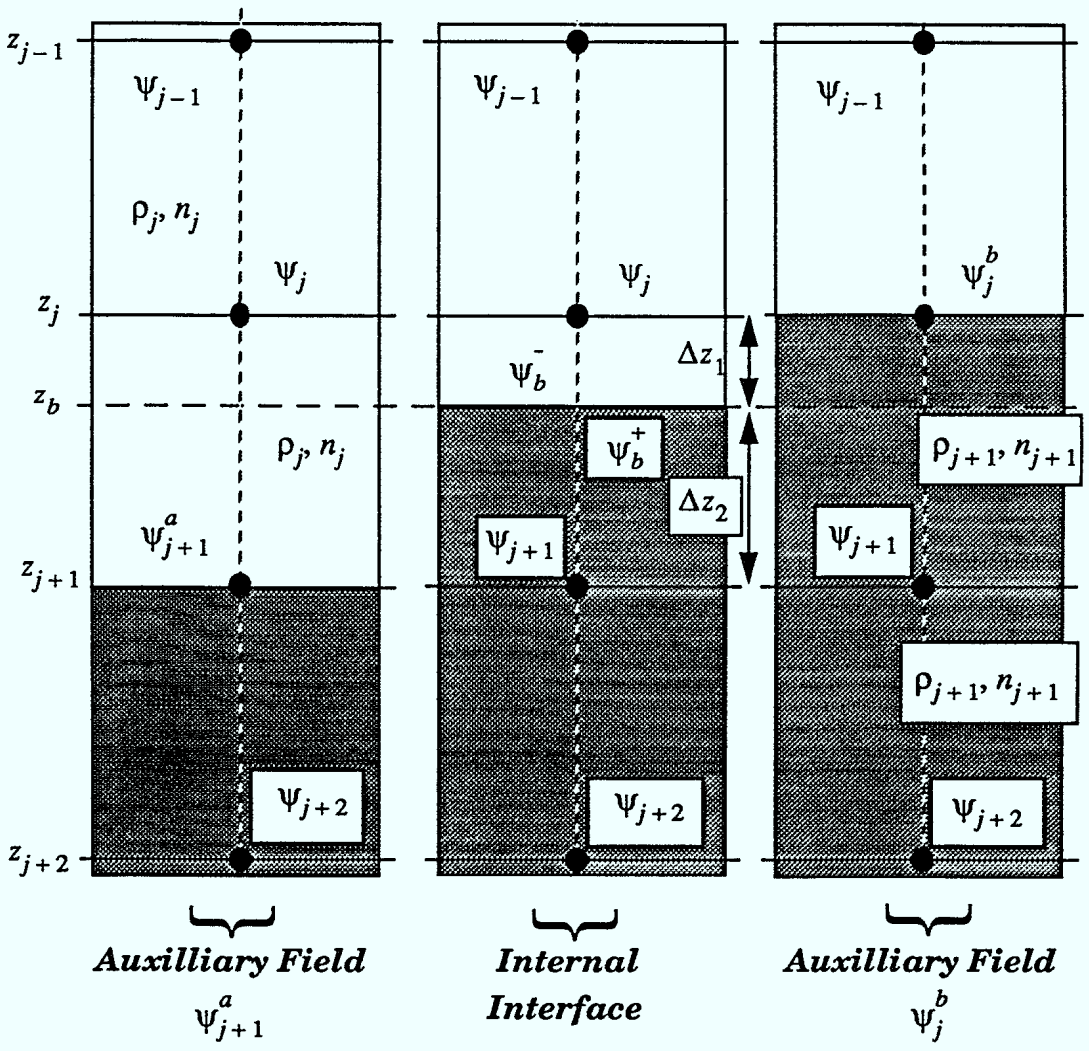

FIGURE 4. Auxilliary PE field definition for an internal interface (second-order). Note that the range subscript has been suppressed.

Thus,

$$\psi^{-}_{1,b} = \frac{1}{2\Delta z^2}\left\{ \Delta z_1 \overline{\Delta z_1}\psi^{a}_{1,j+1} + 2\Delta z_2 \overline{\Delta z_1}\psi_{1,j} - \Delta z_2 \Delta z_1 \psi_{1,j-1} \right\} \tag{47}$$

$$\frac{\partial \psi^{-}_{1,b}}{\partial z} = \frac{1}{2\Delta z^2}\left\{ \{\overline{\Delta z_1} + \Delta z_1\}\psi^{a}_{1,j+1} - 4\Delta z_1 \psi_{1,j} - \overline{\Delta z}\psi_{1,j-1} \right\} \tag{48}$$

and

$$\frac{\partial^2 \psi^{-}_{1,b}}{\partial z^2} = \frac{1}{2\Delta z^2}\left\{ 2\psi^{a}_{1,j+1} - 4\psi_{1,j} + 2\psi_{1,j-1} \right\} \tag{49}$$

where $\overline{\Delta z_1} = \Delta z + \Delta z_1$ and $\overline{\Delta z} = \Delta z_2 - \Delta z_1$.

Similarly, we can define Taylor expansions below the interface as

$$\psi_{1,j+1} = \psi^{+}_{1,b} + \Delta z_2 \frac{\partial \psi^{+}_{1,b}}{\partial z} + \frac{\{\Delta z_2\}^2}{2}\frac{\partial^2 \psi^{+}_{1,b}}{\partial z^2} , \tag{50}$$

$$\psi_{1,j+2} = \psi^{+}_{1,b} + \{\Delta z + \Delta z_2\}\frac{\partial \psi^{+}_{1,b}}{\partial z} + \frac{\{\Delta z + \Delta z_2\}^2}{2}\frac{\partial^2 \psi^{+}_{1,b}}{\partial z^2} \tag{51}$$

and

$$\psi^{b}_{1,j} = \psi^{+}_{1,b} - \Delta z_1 \frac{\partial \psi^{+}_{1,b}}{\partial z} + \frac{\{\Delta z_1\}^2}{2}\frac{\partial^2 \psi^{+}_{1,b}}{\partial z^2} . \tag{52}$$

As before, we can solve equations (50-52) for the three unknown field quantities on the boundary

$$\psi^{+}_{1,b} = \frac{1}{2\Delta z^2}\left\{ \Delta z_2 \overline{\Delta z_2}\psi^{b}_{1,j} + 2\Delta z_1 \overline{\Delta z_2}\psi_{1,j+1} - \Delta z_2 \Delta z_1 \psi_{1,j+2} \right\} , \tag{53}$$

$$\frac{\partial \psi^{+}_{1,b}}{\partial z} = \frac{1}{2\Delta z^2}\left\{ \quad -\{\Delta z_2 + \overline{\Delta z_2}\}\,\psi^{b}_{1,j} + 4\Delta z_2 \psi_{1,j+1} - \overline{\Delta z}\psi_{1,j+2} \quad \right\} \tag{54}$$

and

$$\frac{\partial^2 \psi^{+}_{1,b}}{\partial z^2} = \frac{1}{2\Delta z^2}\left\{ \quad 2\psi^{b}_{1,j} - 4\psi_{1,j+1} + 2\psi_{1,j+2} \quad \right\} \tag{55}$$

where $\overline{\Delta z_2} = \Delta z + \Delta z_2$.

We now proceed by taking equations (47-48) and equations (53-54) in conjunction with equations (32-33) to obtain two equations in the two auxiliary fields

$$\begin{aligned} \Delta z_1 \overline{\Delta z_1}\psi^{a}_{1,j+1} - \Delta z_2 \overline{\Delta z_2}\psi^{b}_{1,j} &= \Delta z_2 \Delta z_1 \psi_{1,j-1} \\ &\quad -2\Delta z_2 \overline{\Delta z_1}\psi_{1,j} + 2\Delta z_1 \overline{\Delta z_2}\psi_{1,j+1} - \Delta z_2 \Delta z_1 \psi_{1,j+2} \end{aligned} \tag{56}$$

and

$$\begin{aligned} \rho_{j+1}\{\Delta z_1 + \overline{\Delta z_1}\}\,\psi^{a}_{1,j+1} + \rho_j\{\Delta z_2 + \overline{\Delta z_2}\}\,\psi^{b}_{1,j} &= \rho_{j+1}\overline{\Delta z}\psi_{1,j-1} \\ &\quad 4\rho_{j+1}\Delta z_1 \psi_{1,j} + 4\rho_j \Delta z_2 \psi_{1,j+1} - \rho_j \overline{\Delta z}\psi_{1,j+2} \end{aligned} \tag{57}$$

Solving for the auxiliary fields yields

$$\psi^{a}_{1,j+1} = \alpha_{j-1}\psi_{1,j-1} + \alpha_j \psi_{1,j} + \alpha_{j+1}\psi_{1,j+1} + \alpha_{j+2}\psi_{1,j+2} \tag{58}$$

and

$$\psi^{b}_{1,j} = \beta_{j-1}\psi_{1,j-1} + \beta_j \psi_{1,j} + \beta_{j+1}\psi_{1,j+1} + \beta_{j+2}\psi_{1,j+2} \tag{59}$$

where

$$\alpha_{j-1} = \frac{1}{\Re}\{\rho_j\{\Delta z_2 + \overline{\Delta z_2}\}\Delta z_2\Delta z_1 + \rho_{j+1}\overline{\Delta z}\Delta z_2\overline{\Delta z_2}\}$$

$$\alpha_j = \frac{1}{\Re}\{-2\rho_j\{\Delta z_2 + \overline{\Delta z_2}\}\Delta z_2\overline{\Delta z_1} + 4\rho_{j+1}\Delta z_1\Delta z_2\overline{\Delta z_2}\}$$

$$\alpha_{j+1} = \frac{1}{\Re}\{2\rho_j\{\Delta z_2 + \overline{\Delta z_2}\}\overline{\Delta z_2}\Delta z_1 + 4\rho_j\Delta z_2\Delta z_2\overline{\Delta z_2}\}$$

$$\alpha_{j+2} = \frac{1}{\Re}\{-\rho_j\{\Delta z_2 + \overline{\Delta z_2}\}\Delta z_2\Delta z_1 - \rho_j\overline{\Delta z}\Delta z_2\overline{\Delta z_2}\} \tag{60}$$

and

$$\beta_{j-1} = \frac{1}{\Re}\{\rho_{j+1}\overline{\Delta z}\Delta z_1\overline{\Delta z_1} - \rho_{j+1}\{\Delta z_1 + \overline{\Delta z_1}\}\Delta z_1\Delta z_2\}$$

$$\beta_j = \frac{1}{\Re}\{4\rho_{j+1}\Delta z_1\Delta z_1\overline{\Delta z_1} + 2\rho_{j+1}\{\Delta z_1 + \overline{\Delta z_1}\}\Delta z_2\overline{\Delta z_1}\}$$

$$\beta_{j+1} = \frac{1}{\Re}\{4\rho_j\Delta z_2\Delta z_1\overline{\Delta z_1} - 2\rho_{j+1}\{\Delta z_1 + \overline{\Delta z_1}\}\Delta z_1\overline{\Delta z_2}\}$$

$$\beta_{j+2} = \frac{1}{\Re}\{-\rho_j\overline{\Delta z}\Delta z_1\overline{\Delta z_1} + \rho_{j+1}\{\Delta z_1 + \overline{\Delta z_1}\}\Delta z_1\Delta z_2\} \tag{61}$$

and where

$$\Re = \rho_j\{\Delta z_2 + \overline{\Delta z_2}\}\Delta z_1\overline{\Delta z_1} + \rho_{j+1}\{\Delta z_1 + \overline{\Delta z_1}\}\Delta z_2\overline{\Delta z_2}\ . \tag{62}$$

Following a similar procedure, we can obtain the equivalent expressions for the auxiliary fields at the advanced range step $x=x_2$. Thus,

$$\psi^a_{2,j+1} = \alpha_{j-1}\psi_{2,j-1} + \alpha_j\psi_{2,j} + \alpha_{j+1}\psi_{2,j+1} + \alpha_{j+2}\psi_{2,j+2} \tag{63}$$

and

$$\psi^b_{2,j} = \beta_{j-1}\psi_{2,j-1} + \beta_j\psi_{2,j} + \beta_{j+1}\psi_{2,j+1} + \beta_{j+2}\psi_{2,j+2}\ . \tag{64}$$

We have derived expressions for the auxiliary fields which depend on the unknown grid point field values. As before, we can substitute equations (58) and (63) directly into

equation (14) (i.e., into equation (40)) to obtain the finite-difference equation for the j^{th} grid point

$$\{m_{1j}^{l} + m_{3j}^{l}\alpha_{j-1}\}\psi_{2,j-1} + \{m_{2j}^{l} + m_{3j}^{l}\alpha_{j}\}\psi_{2,j} + m_{3j}^{l}\alpha_{j+1}\psi_{2,j+1} + m_{3j}^{l}\alpha_{j+2}\psi_{2,j+2} = \{m_{1j}^{r} + m_{3j}^{r}\alpha_{j-1}\}\psi_{1,j-1} + \{m_{2j}^{r} + m_{3j}^{r}\alpha_{j}\}\psi_{1,j} + m_{3j}^{r}\alpha_{j+1}\psi_{1,j+1} + m_{3j}^{r}\alpha_{j+2}\psi_{1,j+2} \quad . \quad (65)$$

Similarly, we can substitute equations (59) and (64) into equation (42) to get the finite-difference equation for the $j+1^{th}$ grid point

$$\{m_{1j}^{l} + m_{3j}^{l}\beta_{j-1}\}\psi_{2,j-1} + \{m_{2j}^{l} + m_{3j}^{l}\beta_{j}\}\psi_{2,j} + m_{3j}^{l}\beta_{j+1}\psi_{2,j+1} + m_{3j}^{l}\beta_{j+2}\psi_{2,j+2} = \{m_{1j}^{r} + m_{3j}^{r}\beta_{j-1}\}\psi_{1,j-1} + \{m_{2j}^{r} + m_{3j}^{r}\beta_{j}\}\psi_{1,j} + m_{3j}^{r}\beta_{j+1}\psi_{1,j+1} + m_{3j}^{r}\beta_{j+2}\psi_{1,j+2} \quad . \quad (66)$$

The preceeding analysis has clearly indicated that it is possible to modify the internal interface corrections to include second-order accurate effects. However, we notice that equations (65) and (66) alter the tridiagonal nature of our marching matrices. Fortunately, it is straightforward to rearrange these two equations to read

$$\overline{m_{1j}^{l}}\psi_{2,j-1} + \overline{m_{2j}^{l}}\psi_{2,j} + \overline{m_{3j}^{l}}\psi_{2,j+1} = \overline{m_{1j}^{r}}\psi_{1,j-1} + \overline{m_{2j}^{r}}\psi_{1,j} + \overline{m_{3j}^{r}}\psi_{1,j+1} + \overline{m_{4j}^{r}}\psi_{1,j+2} \quad (67)$$

and

$$\overline{m_{1j+1}^{l}}\psi_{2,j} + \overline{m_{2j+1}^{l}}\psi_{2,j+1} + \overline{m_{3j+1}^{l}}\psi_{2,j+2} = \overline{m_{1j+1}^{r}}\psi_{1,j-1} + \overline{m_{2j+1}^{r}}\psi_{1,j} + \overline{m_{3j+1}^{r}}\psi_{1,j+1} + \overline{m_{4j+1}^{r}}\psi_{1,j+2} \quad (68)$$

where

$$
\begin{aligned}
\overline{m^{l}_{1j}} &= \{m^{l}_{1j} + m^{l}_{3j}\alpha_{j-1}\}\,\overline{m^{l}_{3j+1}} \\
\overline{m^{l}_{2j}} &= \{m^{l}_{2j} + m^{l}_{3j}\alpha_{j}\}\,\overline{m^{l}_{3j+1}} - m^{l}_{3j}\alpha_{j+2}\overline{m^{l}_{1j+1}} \\
\overline{m^{l}_{3j}} &= m^{l}_{3j}\alpha_{j+1}\overline{m^{l}_{3j+1}} - m^{l}_{3j}\alpha_{j+2}\overline{m^{l}_{2j+1}} \\
\overline{m^{r}_{1j}} &= \{m^{r}_{1j} + m^{r}_{3j}\alpha_{j-1}\}\,\overline{m^{l}_{3j+1}} - m^{l}_{3j}\alpha_{j+2}\overline{m^{r}_{1j+1}} \\
\overline{m^{r}_{2j}} &= \{m^{r}_{2j} + m^{r}_{3j}\alpha_{j}\}\,\overline{m^{l}_{3j+1}} - m^{l}_{3j}\alpha_{j+2}\overline{m^{r}_{2j+1}} \\
\overline{m^{r}_{3j}} &= m^{r}_{3j}\alpha_{j+1}\overline{m^{l}_{3j+1}} - m^{l}_{3j}\alpha_{j+2}\overline{m^{r}_{3j+1}} \\
\overline{m^{r}_{4j}} &= m^{r}_{3j}\alpha_{j+2}\overline{m^{l}_{3j+1}} - m^{l}_{3j}\alpha_{j+2}\overline{m^{r}_{4j+1}}
\end{aligned}
\tag{69}
$$

and

$$
\begin{aligned}
\overline{m^{l}_{1j+1}} &= \{m^{l}_{2j} + m^{l}_{3j}\beta_{j}\}\,\{m^{l}_{1j} + m^{l}_{3j}\alpha_{j-1}\} - \{m^{l}_{2j} + m^{l}_{3j}\alpha_{j}\}\,\{m^{l}_{1j} + m^{l}_{3j}\beta_{j-1}\} \\
\overline{m^{l}_{2j+1}} &= m^{l}_{3j}\beta_{j+1}\{m^{l}_{1j} + m^{l}_{3j}\alpha_{j-1}\} - m^{l}_{3j}\alpha_{j+1}\{m^{l}_{1j} + m^{l}_{3j}\beta_{j-1}\} \\
\overline{m^{l}_{3j+1}} &= m^{l}_{3j}\beta_{j+2}\{m^{l}_{1j} + m^{l}_{3j}\alpha_{j-1}\} - m^{l}_{3j}\alpha_{j+2}\{m^{l}_{1j} + m^{l}_{3j}\beta_{j-1}\} \\
\overline{m^{r}_{1j+1}} &= \{m^{r}_{1j} + m^{r}_{3j}\beta_{j-1}\}\{m^{l}_{1j} + m^{l}_{3j}\alpha_{j-1}\} - \{m^{r}_{1j} + m^{r}_{3j}\alpha_{j-1}\}\{m^{l}_{1j} + m^{l}_{3j}\beta_{j-1}\} \\
\overline{m^{r}_{2j+1}} &= \{m^{r}_{2j} + m^{r}_{3j}\beta_{j}\}\{m^{l}_{1j} + m^{l}_{3j}\alpha_{j-1}\} - \{m^{r}_{2j} + m^{r}_{3j}\alpha_{j}\}\,\{m^{l}_{1j} + m^{l}_{3j}\beta_{j-1}\} \\
\overline{m^{r}_{3j+1}} &= m^{r}_{3j}\beta_{j+1}\{m^{l}_{1j} + m^{l}_{3j}\alpha_{j-1}\} - m^{r}_{3j}\alpha_{j+1}\{m^{l}_{1j} + m^{l}_{3j}\beta_{j-1}\} \\
\overline{m^{r}_{4j+1}} &= m^{r}_{3j}\beta_{j+2}\{m^{l}_{1j} + m^{l}_{3j}\alpha_{j-1}\} - m^{r}_{3j}\alpha_{j+2}\{m^{l}_{1j} + m^{l}_{3j}\beta_{j-1}\}\,.
\end{aligned}
\tag{70}
$$

Thus, it is possible to maintain the tridiagonal form of the left-hand marching matrix, M_L, but not the right-hand matrix, M_R. Since the right-hand matrix is multiplied directly onto a known vector quantity, this fact does not significantly impact on the efficiency of the marching algorithm.

2.6 Sloping Interface Boundary Conditions

Traditionally, the PE is derived on the basis that the waveguide is range independent over each range step. Recently, a procedure has been presented [10] which allows the boundary conditions along a sloping interface to be incorporated into a range-independent PE grid step. Here we demonstrate that the second-order accurate internal interface procedure outlined in the previous section can be used to include effects due to sloping internal interfaces in a straightforward manner. Consider the single range step equivalence shown in Figure 5. The left hand illustration depicts the true sloping interface relative to the PE grid. The right hand illustration indicates how the sloping interface is replaced by a horizontal interface on which modified boundary conditions are applied. The sloping interface conditions are [10] (at $x = x_1$):

$$\psi^{-}_{1,b} = \psi^{+}_{1,b} \tag{71}$$

and

$$\frac{1}{\rho_1}\left\{\frac{\partial \psi^{-}_{1,b}}{\partial z} + A_B \frac{\partial^2 \psi^{-}_{1,b}}{\partial z^2} + B_B^{-} \psi^{-}_{1,b}\right\} = \frac{1}{\rho_2}\left\{\frac{\partial \psi^{+}_{1,b}}{\partial z} + A_B \frac{\partial^2 \psi^{+}_{1,b}}{\partial z^2} + B_B^{+} \psi^{+}_{1,b}\right\} \quad . \tag{72}$$

A corresponding set of conditions hold at $x = x_2$. We define auxiliary field values $\{\psi^{b}_{1,j}, \psi^{a}_{1,j+1}, \psi^{b}_{2,j}, \psi^{a}_{2,j+1}\}$ such that the sloping boundary conditions (equations (71) and (72)) are satisfied along the equivalent horizontal interface. Following the analysis presented previously, the solutions for the auxiliary field values may be written as

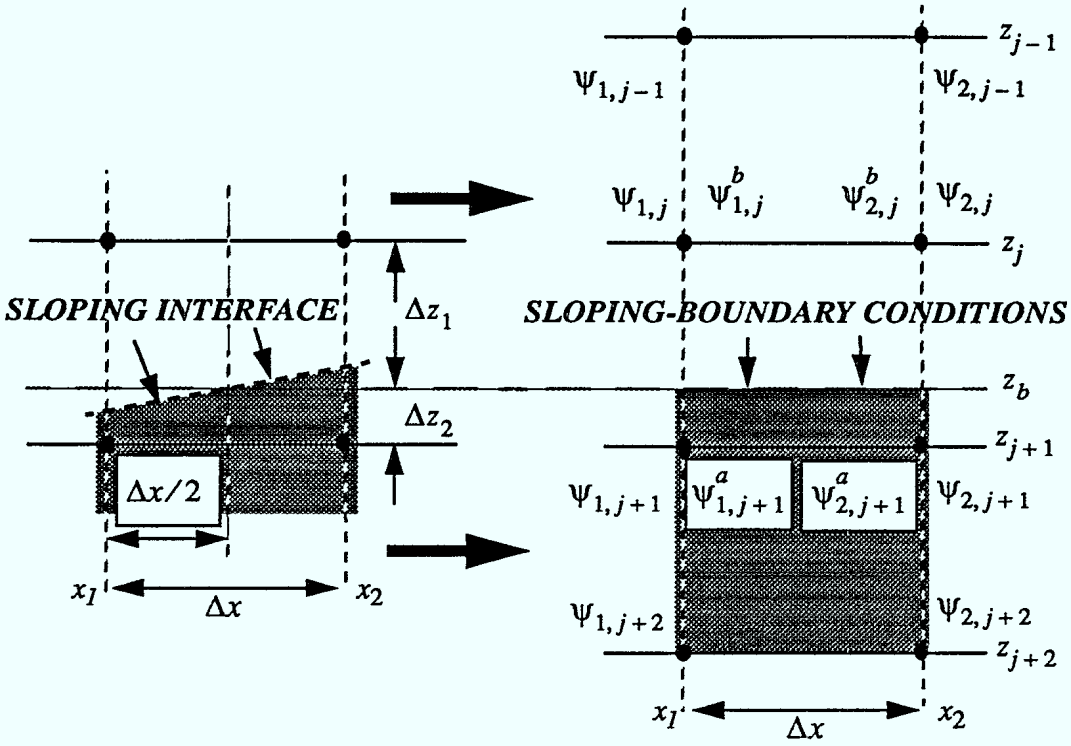

FIGURE 5. Relationship of sloping interface, associated horizontal interface with modifed boundary condition and the PE computational grid points.

$$\psi^a_{1,j+1} = \hat{\alpha}_{j-1}\psi_{1,j-1} + \hat{\alpha}_j\psi_{1,j} + \hat{\alpha}_{j+1}\psi_{1,j+1} + \hat{\alpha}_{j+2}\psi_{1,j+2}\,, \tag{73}$$

$$\psi^b_{1,j} = \hat{\beta}_{j-1}\psi_{1,j-1} + \hat{\beta}_j\psi_{1,j} + \hat{\beta}_{j+1}\psi_{1,j+1} + \hat{\beta}_{j+2}\psi_{1,j+2}\,, \tag{74}$$

$$\psi^a_{2,j+1} = \hat{\alpha}_{j-1}\psi_{2,j-1} + \hat{\alpha}_j\psi_{2,j} + \hat{\alpha}_{j+1}\psi_{2,j+1} + \hat{\alpha}_{j+2}\psi_{2,j+2} \tag{75}$$

and

$$\psi^b_{2,j} = \hat{\beta}_{j-1}\psi_{2,j-1} + \hat{\beta}_j\psi_{2,j} + \hat{\beta}_{j+1}\psi_{2,j+1} + \hat{\beta}_{j+2}\psi_{2,j+2}\,. \tag{76}$$

In equations (73-76) we have

$$\hat{\alpha}_{j-1} = \frac{1}{\varnothing}\Big(\Re\alpha_{j-1} - \rho_j \{2A_B + B_B^b \Delta z_2 \overline{\Delta z_2}\} \Delta z_2 \Delta z_1 - \rho_{j+1} \Delta z_2 \overline{\Delta z_2} \{2A_B - B_B^a \Delta z_2 \Delta z_1\} \Big)$$

$$\hat{\alpha}_j = \frac{1}{\varnothing}\Big(\Re\alpha_j + 2\rho_j \{2A_B + B_B^b \Delta z_2 \overline{\Delta z_2}\} \Delta z_2 \overline{\Delta z_1} + \rho_{j+1} \Delta z_2 \overline{\Delta z_2} \{4A_B - 2B_B^a \Delta z_2 \overline{\Delta z_1}\} \Big)$$

$$\hat{\alpha}_{j+1} = \frac{1}{\varnothing}\Big(\Re\alpha_{j+1} + 2\rho_j \{2A_B + B_B^b \Delta z_2 \overline{\Delta z_2}\} \overline{\Delta z_2} \Delta z_1 - \rho_j \Delta z_2 \overline{\Delta z_2} \{4A_B - 2B_B^b \overline{\Delta z_2} \Delta z_1\} \Big)$$

$$\hat{\alpha}_{j+2} = \frac{1}{\varnothing}\Big(\Re\alpha_{j+2} + \rho_j \{2A_B + B_B^b \Delta z_2 \overline{\Delta z_2}\} \Delta z_2 \Delta z_1 - \rho_j \Delta z_2 \overline{\Delta z_2} \{2A_B - B_B^b \Delta z_2 \Delta z_1\} \Big) \quad (77)$$

and

$$\hat{\beta}_{j-1} = \frac{1}{\varnothing}\Big(\Re\beta_{j-1} - \rho_{j+1} \overline{\Delta z_1} \Delta z_1 \{2A_B - \Delta z_1 \Delta z_2 B_B^a\} - \rho_{j+1} \Delta z_1 \Delta z_2 \{2A_B + \Delta z_1 \overline{\Delta z_1} B_B^a\} \Big)$$

$$\hat{\beta}_j = \frac{1}{\varnothing}\Big(\Re\beta_j + \rho_{j+1} \Delta z_1 \overline{\Delta z_1} \{2A_B - \overline{\Delta z_1} \Delta z_2 B_B^a\} + 2\rho_{j+1} \Delta z_2 \overline{\Delta z_1} \{2A_B + \Delta z_1 \overline{\Delta z_1} B_B^a\} \Big)$$

$$\hat{\beta}_{j+1} = \frac{1}{\varnothing}\Big(\Re\beta_{j+1} - \rho_j \Delta z_1 \overline{\Delta z_1} \{4A_B - 2\Delta z_1 \overline{\Delta z_2} B_B^b\} - 2\rho_{j+1} \Delta z_1 \overline{\Delta z_2} \{2A_B + \Delta z_1 \overline{\Delta z_1} B_B^a\} \Big)$$

$$\hat{\beta}_{j+2} = \frac{1}{\varnothing}\Big(\Re\beta_{j+2} + \rho_j \Delta z_1 \overline{\Delta z_1} \{2A_B - \Delta z_1 \Delta z_2 B_B^b\} + 2\rho_{j+1} \Delta z_1 \Delta z_2 \{2A_B + \Delta z_1 \overline{\Delta z_1} B_B^a\} \Big) \quad (78)$$

where

$$\varnothing = \Re - \rho_j \{2A_B + B_B^b \Delta z_2 \overline{\Delta z_2}\} \Delta z_1 \overline{\Delta z_1} + \rho_{j+1} \{2A_B + B_B^a \Delta z_2 \overline{\Delta z_1}\} \Delta z_2 \overline{\Delta z_2} \ . \quad (79)$$

From this point we can proceed by substituting equations (73-76) directly into equations (40) and (42) and then carry out the identical retridiagonalization procedure defined by equations (67-70).

In summary, we have approximated the effect of a sloping internal interface by incorporating a modified boundary condition along an associated horizontal internal interface. The second-order accurate internal interface analysis has been used to derive a set of straightforward modifications to the existing PE marching matrices.

3.0 Numerical Results

In this section we apply the preceding analysis to three numerical test cases. First, we use a relatively shallow-water range-independent application [11] to test both the first and second-order internal interface analysis. This application also demonstrates the potential sensitivity of matched-field processing to bathymetry in shallow water, and hence, the significance of internal interfaces to modelling applications. Second, we consider an Arctic application involving bathymetries typical of the continental-shelf edge (~500 m) - in this problem, internal interfaces are a relatively insignificant problem. Third, we use the ASA Benchmark Wedge problem [12] to demonstate the application of the range-dependent internal interface analysis.

3.1 A Shallow Water Example

Consider the waveguide configuration shown in Figure 6(a). An isospeed water column, 120 m deep, with a sound speed of 1.494 km/s overlays an isospeed sedimentary basement with a sound speed of 1.600 km/s. A source is placed at mid-depth at 60 m. Propagation loss as a function of range to a shallow receiver at a depth of 30 m is shown as the solid curve in Figure 6(b) for a source frequency of 30 Hz. For comparison, propagation loss to the same receiver but for a water depth of 119 m is shown as the

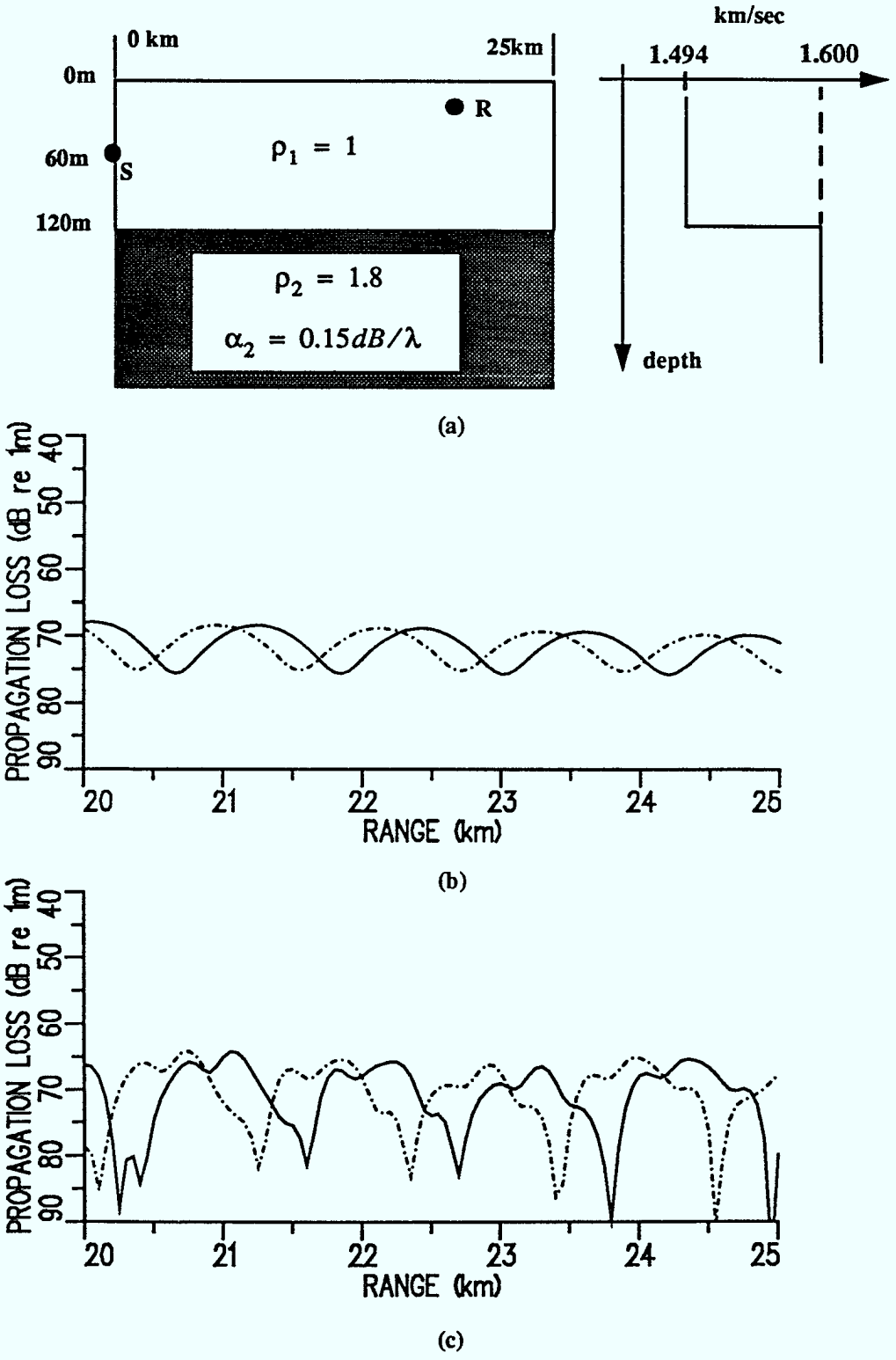

FIGURE 6. (a) Shallow water waveguide configuration R=30 m, (b) propagation loss (f=30 Hz) for water depth of 120 m(———) and 119 m (–·–·–), and (c) same for f=100 Hz.

dot-dashed curve. The 1 m discrepancy in water depth effectively translates to a 500m discrepancy in range as indicated by Figures 6(b) and (c); bathymetry can have a significant effect on the phase of the received signal as was noted previously [11] for a related problem. Identical results are shown for a higher frequency of 100 Hz in Figure 6(c). Once again, the 1 m shift in bathymetry causes significant phase shifting over a 25 km range. Not surprisingly, Reference 11 noted that bathymetry was a very significant parameter in matched field applications which employed this waveguide configuration. This example can also be used to demonstrate the numerical application of the internal interface procedure. Propagation loss to the receiver at a depth of 30 m is plotted as a function of range in Figure 7 for a water depth of 119.6 m. Three results, computed at a frequency of 30 Hz, are displayed in this figure. The solid curve is the reference solution provided by the Fast-Field program SAFARI [3]. The dot-dash result was obtained by using the first-order internal interface procedure described earlier. The second-order internal interface results are given as the dotted curve. Good agreement with the reference solutions would indicate that the internal interface procedures yield accurate results (the second-order solution is more accurate as expected).

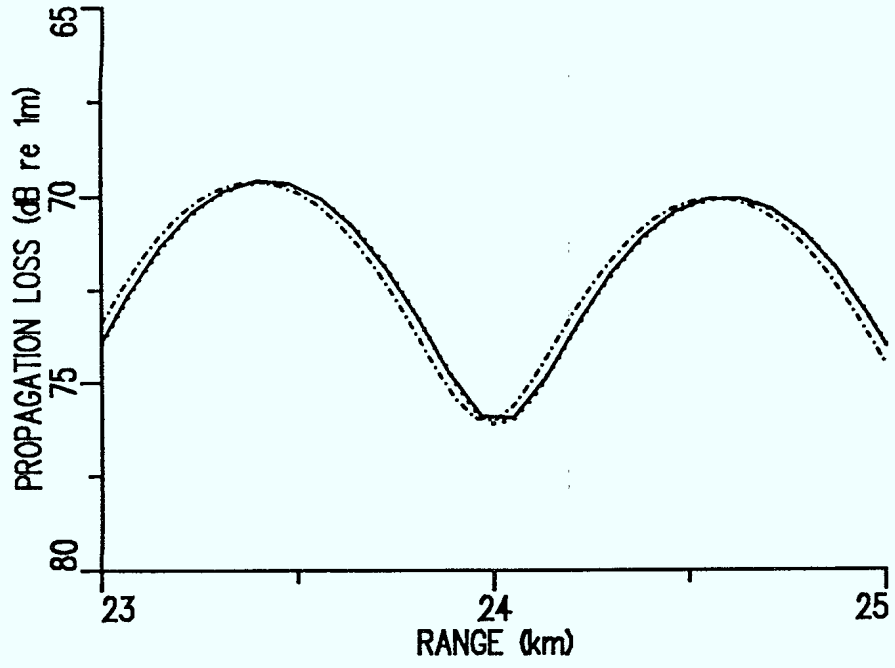

FIGURE 7. Comparison of first (–·–·–) and second(·····) order internal interface solutions with SAFARI result(———). Shallow water application with water depth equal to 119.6 m.

3.2 An Arctic Example

Consider the Arctic waveguide configuration (shown in Figure 8(a)) consisting of an upward refracting ocean, 520 m deep, over a 60 m sediment layer, over an upward-refracting basement. Propagation loss between a source (25 Hz) at 60m and a receiver located at a depth of 100 m is shown as the solid curve in Figure 8(b). For comparison,

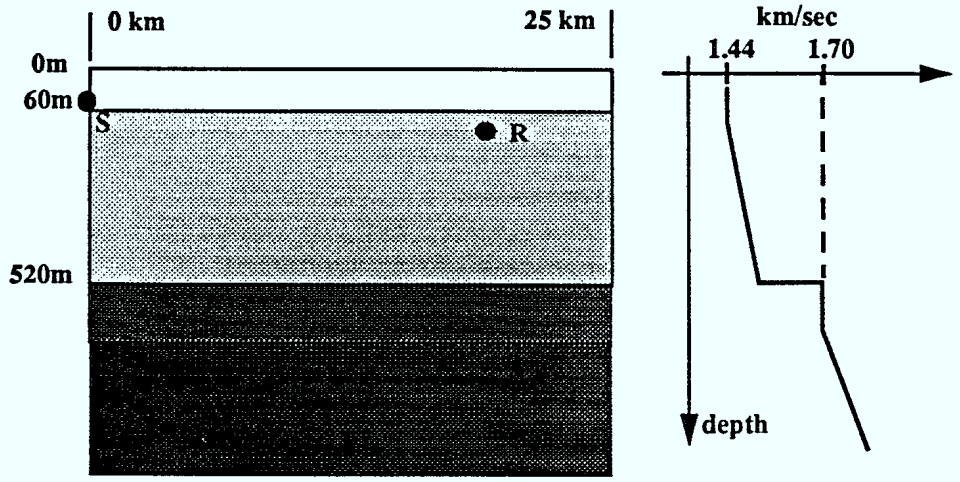

(a)

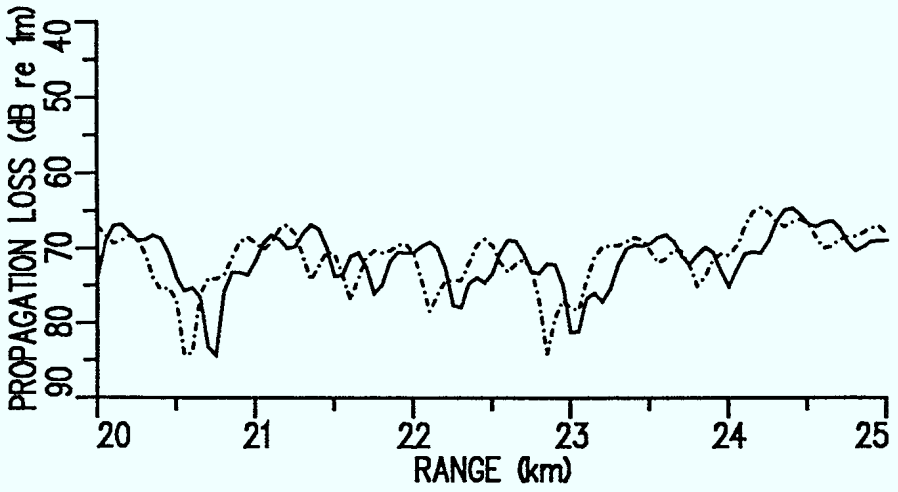

(b)

FIGURE 8. Arctic application: (a) waveguide configuration (R=60 m) and (b) propagation loss versus range for water depths of 520 m (———) and 518 m (·····).

the same characteristic for a water depth of 518 m is shown as the dotted curve. A range-depth grid of 10 m to 2 m, respectively, was employed in the PE calculations. Note that, in contrast to the previous example, the change in water depth does not seriously alter the propagation loss characteristic (i.e., the 2 m bathymetry change resulted in only a 250 m discrepancy in range). The same behaviour is observed at higher frequencies as well (results not shown here) - thus, it is expected that in water depths greater than roughly 500 m, extremely long-range propagation would be necessary in order for an uncertainty in water-bottom interface position (to within a grid width) to have a significant effect.

3.3 A Range-Dependent Example

In this section we use the internal interface analysis for sloping interfaces to examine the sensitivity of the acoustic field in the ASA Benchmark Wedge problem to the manner in which the sloping interface is approximated in the range-updating procedure. The waveguide configuration is shown in Figure 9(a). The staircase approximation to the sloping water/bottom interface is shown in Figure 9(b) relative to the PE range and depth grid for both (i) the standard application of range-updating whereby the staircase is assigned to the nearest grid depth (dashed), and (ii) the internal sloping interface approximation (dotted) described earlier in this paper. Clearly, the internal interface representation is closer to the true interface. Propagation loss results for the Benchmark wedge are shown in Figure 9(c) for a shallow receiver at 30 m. The solid curve is the reference solution generated by Two-Way PE [6], the dashed curve corresponds to the propagation loss obtained when the internal interface approximation described in this paper is used, and finally, the dotted curve is a result obtained using an internal-interface procedure whereby the sloping interface conditions are applied along the standard staircase (SLOPE PE [10]). The dashed and the dotted curves are indistiguishable on the scale chosen. This indicates that the wedge problem is not very sensitive to the nature of the staircase approximation - at least, at a frequency of 25 Hz. This finding also is consistent with the range-independent results shown previously which indicated that at short ranges, the position of the interface internal to the PE grid had negligible effect (i.e., only at longer ranges of 20-25 km were we able to see significant phase shifts).

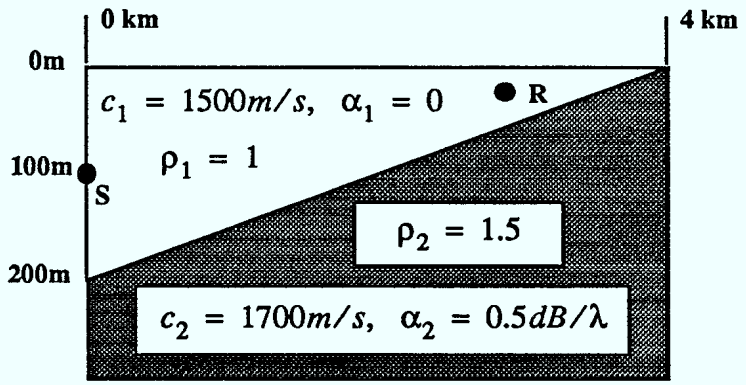

(a)

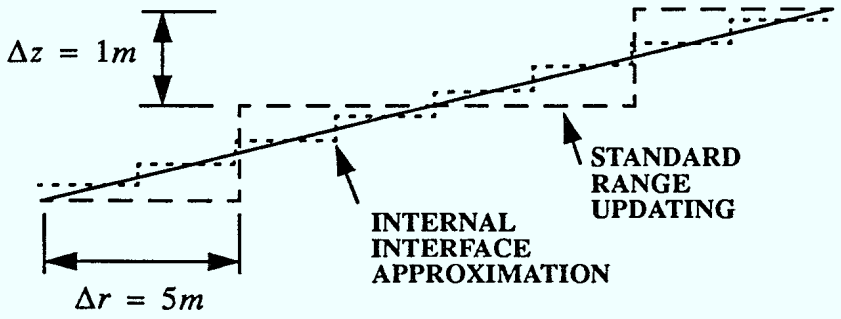

(b)

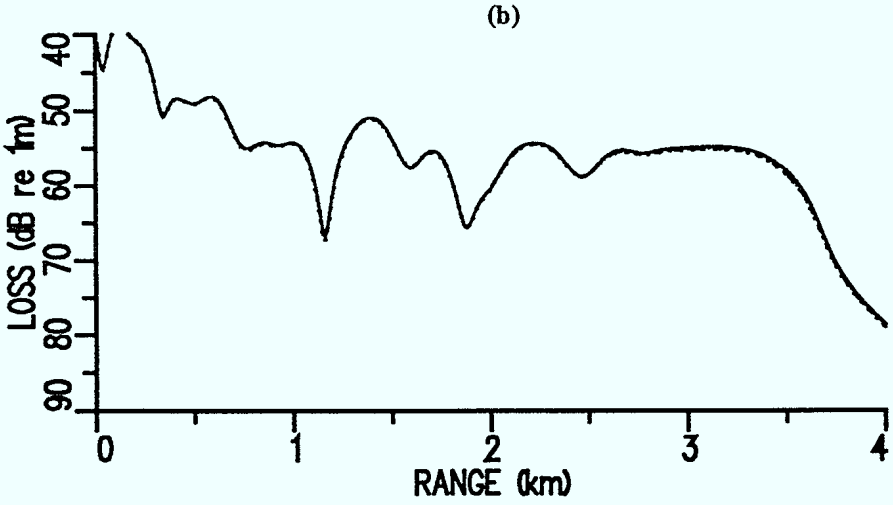

(c)

FIGURE 9. ASA Benchmark Wedge: (a) waveguide configuration, (b) staircase approximations, and (c) propagation loss versus range for Two-Way PE (———), Slope PE (·····), and Internal-Interface PE (–·–·–).

4.0 Summary

An analysis has been presented which outlines how layer interfaces internal to the PE computational grid may be accounted for within the context of a Finite-Difference PE algorithm. Both first- and second-order approximations have been considered. Essentially, the internal interface boundary conditions are satisfied by defining auxiliary field quantities at the regular PE grid points just above and below the interface. Numerically, the procedure is efficient because additional computations added to the PE numerical algorithm are local to the internal interface position. Furthermore, consideration of second-order conditions allows sloping internal interfaces to be easily accomodated. Numerical test cases are used to demonstrate the significance of the analysis - only at ranges greater than 10-20 km in shallow water are internal interfaces likely to be significant in practical applications. It is worth commenting further that the range shift in the acoustic field caused by imprecision in the depth of the ocean bottom (as shown in the numerical examples) is really an upper bound on potential mismatch in MFP applications. In other words, MFP is designed to find the best match according to a criteria involving several parameters; thus, inaccuracy in one of the parameters (i.e., range) can be compensated for, artificially, by allowing slight adjustments in other parameter values that may also be accurate only to within some specified tolerance.

5.0 References

1. M.D. Collins and E.K. Westwood, "A higher-order energy-conserving parabolic equation for range-dependent ocean depth, sound speed, and density," J. Acoust. Soc. Am. **89**, 1068-1075 (1991).

2. R.B. Evans, "A coupled mode solution for acoustic propagation in a waveguide with stepwise depth variations of a penetrable bottom," J.Acoust. Soc. Am. **74**, 188-195 (1983).

3. H. Schmidt and F.B. Jensen, "Efficient numerical solution technique for wave propagation in horizontally stratified ocean environments," Rep. SM-173, SACLANTCEN Technical Publication (1984).

4. R.R. Greene, "A high-angle one-way wave equation for seismic wave propagation along rough and sloping interfaces," J. Acoust. Soc. Am. **77**, 1991-1998 (1985).

5. M.D. Collins, "A higher-order parabolic equation for wave propagation in an ocean overlying an elastic bottom," J. Acoust. Soc. Am. **86**, 1459-1464 (1989).

6. G.H. Brooke and D.J. Thomson, "A single-scatter formalism for improving PE calculations in range-dependent media," in ***PE Workshop II*** edited by S.A. Chin-Bing, D.B. King, J.A. Davis and R.B. Evans, NRL Technical Pubication (1993).

7. A.R. Mitchell, ***Computational Methods in Partial Differential Equations*** (Wiley, London, 1969)

8. F.D. Tappert, "The parabolic approximation method," in ***Wave Propagation and Underwater Acoustics*** edited by J.B. Keller and J.S. Papadakis, Lecture Notes in Physics, Vol. 70 (Springer-Verlag, New York, 1977).

9. M.D. Collins, "A self-starter for the parabolic equation method," J. Acoust. Soc. Am. **92**, 2069-2074 (1992).

10. G.H. Brooke, D.J. Thomson and P.M. Wort, "A sloping-boundary condition for efficient PE calculations in range-dependent acoustic media," J. Comp. Acoustics, submitted for publication.

11. R.M. Hamson and R.M. Heitmeyer,"Environmental and system effects on source localization in shallow water by the matched-field processing of a vertical array," J. Acoust. Soc. Am. **86**, 1950-1959 (1989).

12. F. Jensen and C.M. Ferla, "Numerical solution or range-dependent benchmark problems in ocean acoustics," J. Acoust. Soc. Am. **87**, 1499-1510 (1990).

Distribution

Report: DREP Technical Memorandum 94-145

Title: Internal Interface Conditions for Finite-Difference PE Applications in Layered Acoustic Media

Author: Gary H. Brooke and Philip M. Wort

Date: December 1994

Security: Unclassified

1 - DSIS

9 - DREP

- Library
- Dr. G. Brooke (8)

5 - MacDonald, Dettwiler and Associates Ltd.
13800 Commerce Parkway
Richmond, BC V6V 2J3
Attn: Dr. P. Wort

2 - SACLANT Undersea Research Centre
APO New York, NY 09019-5000
Attn: Dr. F. Jensen, Dr. J. Fawcett

1 - SAIC
#2 Shaw's Cove
Ste. 203
New London, CT 06359
Attn: Dr. R. Evans

1 - Research Centre of Crete
Institute of Applied and Computational Mathematics
PO Box 1527
711 10 Heraklion, Crete, Greece
Attn: Prof. J.S. Papadakis, Director

1 - National Defence Research Establishment
S-17290 Sundbyberg, Sweden
Attn: Dr. I. Karasalo

1 - Yale University
Dept. of Computer Science
PO Box 2158 Yale Station
NewHaven, Conn 06520-2158
Attn: Dr. Ding Lee

1 - Naval Research Laboratory
Code 5160
Washington, DC 20375-5000
Attn: Dr. M. Collins

DOCUMENT CONTROL DATA

(Security classification of title, body of abstract and indexing annotation must be entered when the overall document is classified)

1. ORIGINATOR (the name and address of the organization preparing the document. Organizations for whom the document was prepared, e.g. Establishment sponsoring a contractor's report, or tasking agency, are entered in section 8.)

DREP
FMO Victoria, BC V0S 1B0

2. SECURITY CLASSIFICATION (overall security classification of the document. including special warning terms if applicable)

UNCLAS

3. TITLE (the complete document title as indicated on the title page. Its classification should be indicated by the appropriate abbreviation (S,C,R or U) in parentheses after the title.)

Internal Interface Conditions for Finite-Difference PE Applications in Layered Media

4. AUTHORS (Last name, first name, middle initial)

Gary H. Brooke and Philip M. Wort

5. DATE OF PUBLICATION (month and year of publication of document)

December 1994

6a. NO. OF PAGES (total containing information. Include Annexes, Appendices, etc.)

32

6b. NO. OF REFS (total cited in document)

12

7. DESCRIPTIVE NOTES (the category of the document, e.g. technical report, technical note or memorandum. If appropriate, enter the type of report, e.g. interim, progress, summary, annual or final. Give the inclusive dates when a specific reporting period is covered.)

Technical Memorandum

8. SPONSORING ACTIVITY (the name of the department project office or laboratory sponsoring the research and development. Include the address.)

NA

9a. PROJECT OR GRANT NO. (if appropriate, the applicable research and development project or grant number under which the document was written. Please specify whether project or grant)

NA

9b. CONTRACT NO. (if appropriate, the applicable number under which the document was written)

NA

10a. ORIGINATOR'S DOCUMENT NUMBER (the official document number by which the document is identified by the originating activity. This number must be unique to this document.)

TM 94-145

10b. OTHER DOCUMENT NOS. (Any other numbers which may be assigned this document either by the originator or by the sponsor)

NA

11. DOCUMENT AVAILABILITY (any limitations on further dissemination of the document, other than those imposed by security classification)

(X) Unlimited distribution
( ) Distribution limited to defence departments and defence contractors; further distribution only as approved
( ) Distribution limited to defence departments and Canadian defence contractors; further distribution only as approved
( ) Distribution limited to government departments and agencies; further distribution only as approved
( ) Distribution limited to defence departments; further distribution only as approved
( ) Other (please specify):

12. DOCUMENT ANNOUNCEMENT (any limitation to the bibliographic announcement of this document. This will normally correspond to the Document Availabilty (11). However, where further distribution (beyond the audience specified in 11) is possible, a wider announcement audience may be selected.)

NONE

13. ABSTRACT (a brief and factual summary of the document. It may also appear elsewhere in the body of the document itself. It is highly desirable that the abstract of classified documents be unclassified. Each paragraph of the abstract shall begin with an indication of the security classification of the information in the paragraph (unless the document itself is unclassified) represented as (S), (C), (R), or (U). It is not necessary to include here abstracts in both offical languages unless the text is bilingual).

The traditional one-way parabolic equation (PE) formulation for range-dependent layered acoustic media is modified to include effects associated with interfaces internal to the computational grid. Both first- and second-order approximations are derived which effectively translate the effects of internal boundary conditions onto nearby grid points. The approximations are based on a procedure presented by Collins [J. Acoust. Soc. Am., 86 (1989), 1459-1464] in which auxiliary field variables are definedabove and below the interface. Consideration of second-order conditions also allows sloping internal interfaces to be accommodated. Numerical results obtained for standard test cases are used to demonstrate the application of the analysis. In shallow water, particularly at ranges greater than 20 km, there is an indication that precise definition of the interface depth is required in order to minimize errors that could negatively affect matched field processing applications. Alternatively, imprecision in interface location to within one computational grid width does not significantly affect the field prediction in oceans with water depths greater than 500 m or so.

14. KEYWORDS, DESCRIPTORS or IDENTIFIERS (technically meaningful terms or short phrases that characterize a document and could be helpful in cataloguing the document. They should be selected so that no security classification is required. Identifiers, such as equipment model designation, trade name, military project code name, geographic location may also be included. If possible keywords should be selected from a published thesaurus. e.g. Thesaurus of Engineering and Scientific Terms (TEST) and that thesaurus-identified. If it is not possible to select indexing terms which are Unclassified, the classification of each should be indicated as with the title.)

Acoustic propagation, PE, parabolic equation, finite-differnces, matched-field processing